CONFIDENTIAL

Copy
RM L56A25a

NACA

RESEARCH MEMORANDUM

EFFECT OF FUSELAGE AIR BRAKES ON THE LONGITUDINAL STABILITY CHARACTERISTICS OF A SWEPT-WING FIGHTER MODEL AT TRANSONIC SPEEDS

By Donald D. Arabian

Langley Aeronautical Laboratory
Langley Field, Va.

CLASSIFIED DOCUMENT

NATIONAL ADVISORY COMMITTEE
FOR AERONAUTICS

WASHINGTON

April 24, 1956

CONFIDENTIAL

NATIONAL ADVISORY COMMITTEE FOR AERONAUTICS

RESEARCH MEMORANDUM

EFFECT OF FUSELAGE AIR BRAKES ON THE LONGITUDINAL STABILITY CHARACTERISTICS OF A SWEPT-WING FIGHTER MODEL AT TRANSONIC SPEEDS

By Donald D. Arabian

SUMMARY

An investigation was conducted on a 40° swept-wing fighter model at transonic speeds to determine the effect of extending a fuselage-type air brake located near the wing trailing edge. Force and moment data and wing pressures are presented for a range of Mach numbers and angles of attack. The results indicated that the increment of drag coefficient due to the extended brakes was about 0.03 up to a Mach number of about 0.94 and decreased up to a Mach number of 1.0. The effectiveness of the air brakes was reduced because of their proximity to the wing. The change of the longitudinal stability with extended air brakes required stabilizer changes of ±1° or less for maintaining a trimmed lift coefficient.

INTRODUCTION

Air brakes have become an accepted and often essential control device on present-day clean-design jet-powered airplanes, providing additional maneuvering ability as well as a safe means of reducing speed. Future high-speed jet-powered transports may likewise employ air brakes in order to exploit fully their performance possibilities. The increases in drag that result from the use of air brakes have been measured in wind tunnels and flight tests for a large variety of brakes. Many of these data are summarized in reference 1. The design and location of air brakes as a speed control should have little or no effect on the airplane forces and moments other than to increase the drag when the brakes are extended. Restrictions therefore must be placed on the locations of various type brakes. One of these locations which may be acceptable is an air brake attached to the fuselage close behind the wing trailing edge as found in this investigation. The geometry was

chosen so that the drag increment due to the extended brakes was of the order presently employed on airplanes. The transonic data presented include pressure measurements on the wing as well as force and moment data for a swept-wing fighter model with closed brakes and with the brakes extended about the hinge line 56°. The longitudinal and lateral static stability characteristics of the model with closed brakes are presented in reference 2.

SYMBOLS

$\bar{c}$ mean aerodynamic chord, ft

b wing span, ft

C_D drag coefficient, $\frac{\text{Drag}}{qS}$

ΔC_D incremental drag coefficient due to extended air brakes

C_L lift coefficient, $\frac{\text{Lift}}{qS}$

C_m pitching-moment coefficient, $\frac{\text{Pitching moment}}{qS\bar{c}}$

S wing area, sq ft

q_∞ free-stream dynamic pressure, lb/sq ft

M Mach number

α angle of attack (measured with respect to fuselage reference), deg

δ_{i_t} stabilizer deflection (positive deflection down), deg

$\Delta\delta_{i_t}$ increment of stabilizer deflection for trimmed flight

C_p pressure coefficient, $\frac{p - p_\infty}{q_\infty}$

p local static pressure, lb/sq ft

p_∞ free-stream static pressure, lb/sq ft

MODEL AND TESTS

Model

The general arrangement of the swept-wing fighter model is shown in figure 1. The geometry of the wing was as follows: aspect ratio 3.43, taper ratio 0.578, quarter-chord line sweep 40°, and NACA 64A010 airfoil sections normal to the quarter chord. The incidence of the wing was 1.5° with respect to the fuselage reference line. The wing incorporated two modifications: two fences were installed on each wing panel, and the leading edge outboard of the outermost fence was modified which is characterized principally by having double the leading-edge radius of the basic airfoil section. The wing inlets were ducted to expel air around the sting through the tail pipe.

A detail sketch of the air brakes is shown in figure 2. The leading edges of the brakes were located 0.23 foot aft of the trailing-edge fuselage intersection on each side of the fuselage. The sum of the plan-view areas of both brakes if unperforated would be 0.26 square foot or about 4 percent of the wing area. The total perforated area is 0.04 square foot. The method of attaching the flap in the extended position is shown in the rear-view photograph of figure 3.

A typical photograph of the model with closed brakes mounted in the 16-foot tunnel is shown in figure 4.

Tests

The tests were conducted in the Langley 16-foot transonic tunnel for a Mach number range from 0.80 to 1.05 which corresponded to a Reynolds number range from about 5.1×10^6 to 5.4×10^6 based on the wing mean aerodynamic chord. The angle of attack was varied from -2° to 8° for most of the Mach number range. The model was tested with the air brakes extended (rotated forward 56° about the hinge line) and closed. A horizontal-tail setting of 0° with respect to the fuselage reference line was used for this investigation.

The forces and moment were measured by a strain-gage balance which was mounted internally. The data were corrected by adjusting the base pressure to free-stream static pressure and by subtracting the internal drag. The balance data are presented with respect to the 21-percent mean aerodynamic chord. The angle of attack was measured with respect to the fuselage reference line. Wing pressure measurements were made at the spanwise stations of 22.8, 37.6, and 74 percent of the semispan for the upper and lower chordwise stations of 1.25, 2.5, 5, 10, 20, 30, 40, 50, 60, 70, 75, 80, 85, 90, and 95 percent of the chord.

RESULTS

The force and moment data are presented as coefficients in figure 5 for the closed and extended air brakes over the tested Mach number range. In general, the results showed that for most of the angles of attack, the extended air brakes reduced the lift coefficient. There was an abrupt change in the slope of the lift curve near an angle of attack of 0° for Mach numbers of 0.98 and higher. The increment of drag coefficient is best shown in figure 6(a) for lift coefficients at 0 and 0.3. The incremental drag coefficient was about 0.03 up to a Mach number of about 0.94 and then decreased to about 0.02 near Mach number 1.00. The drag coefficient for an equivalent projected flat-plate area of the brakes based on the wing area would be approximately 0.045. The changes in the static longitudinal stability were generally small except close to zero lift coefficient at Mach numbers of 0.98 and higher where instability was indicated for a very small range of lift coefficient.

DISCUSSION

The results can be explained best by a study of what happens to the wing pressures when the brakes are extended. In figure 7, a comparison of the chordwise pressure distributions for the closed and extended air brakes is presented for angles of attack of -2°, 0°, and 4° and for Mach numbers of 0.90, 098, and 1.03. These conditions are sufficient to furnish representative pressure distributions for the investigation.

The change of the lift-curve slopes of figure 5 was mainly associated with the change of the relative position of the predominant shock on the upper- and lower-wing surfaces. This characteristic will be noted in figure 7 for the 22.8- and 37.6-percent semispan wing stations for the Mach numbers of 0.98 and 1.03. For both of these Mach numbers at an angle of attack of -2° the chordwise location of the lower-surface shock was ahead of the upper-surface shock so that positive normal force occurs over a portion of the chord between these shocks with the air brakes extended. With the brakes closed the position of the predominant upper- and lower-surface shocks was such that there was either a small negative or essentially no normal force over the portion of the chord near the shocks. Since the normal loading on the remaining portions of the chord for both configurations was approximately the same for speed brakes extended or closed, the total lift was therefore higher for the model with the extended brakes. The same respective location of the shocks occurred for an angle of attack of -1° although not presented. Increasing the angle of attack to 0° caused the

upper- and lower-surface shock locations to coincide approximately with each other at the 22.8- and 37.6-percent semispan station. As a result, the lift decreased and became zero or slightly negative for the length of chord near the shock waves. This decrease of lift due to the shift of the upper- and lower-surface shocks roughly cancelled the increase of lift over the remaining portion of the chord resulting from the increase of angle of attack, so that effectively the lift slope decreased. A further increase of angle of attack to 4° shows the lower-surface shock to shift aft of the upper-surface shock wave for the same two semispan stations. Thus, negative lift was produced over the chord length between the two shocks. However, aft of the lower-surface shock lift increases at a greater rate with angle of attack than the losses resulting from the shift of the shock waves. Therefore, the slope of the lift curve increased and actually became somewhat greater than the lift slope for the closed brake configuration.

Probably the most significant factor to be noted in considering the drag or effectiveness of the air brakes was their effect on the magnitude of the pressures on the aft portion of the wing (fig. 7). The proximity of the brakes to the wing caused a more positive pressure to exist on the aft portion of the wing with extended brakes than with closed brakes. The more positive pressure resulted in a decrease of the wing drag and an obscured reduction of the air-brake effectiveness at all Mach numbers. Apparently, a more effective brake could be obtained by locating the brake away from its present location behind the wing trailing edge. There is, however, a Mach number effect indicated by the wing pressures. A study of the changes of the wing pressure distributions for Mach numbers of 0.90 and 0.98 indicated that a greater increase of pressure on the aft portion of the wing occurred when the air brakes were extended at the higher Mach number. Therefore, the reduction in wing drag arising from the greater increased pressures at a Mach number of 0.98 resulted in less effectiveness of the air brake as shown in figure 6(a). For the Mach numbers above 0.98 the change in the wing pressures when the brakes were extended was found to be such as to decrease slightly the reduction of effectiveness of the brakes.

The static longitudinal instability shown in figure 5 at low lift coefficients was a result of the shock (wave) locations on the upper and lower surfaces of the wing explained in the discussion of the lift curve. Although the test range did not include lift coefficients above 0.7, there is a possibility that longitudinal instability would occur at higher C_L values for the model with extended air brakes compared to the closed brake configuration as evidenced by the data of $M = 0.94$.

The force data indicated some change of the airplane attitude would result from extending the air brakes. A study of figure 5 shows the angle of attack for trim will, in general, increase about 1° at most with the extension of the brakes. A slight additional change in the attitude will result from the change in stabilizer setting necessary to trim with extended brakes. The change in stabilizer setting required to maintain a trimmed lift coefficient of 0.2 and 0.3 for the tested Mach number range is shown in figure 6(b) (the necessary tail characteristics were obtained from reference 3 with the additional assumption that the stabilizer effectiveness is unchanged with brake extension). Stabilizer changes of about ±1° or less are shown. Down-stabilizer deflections are required for the Mach numbers less than about 0.96 while up-stabilizer deflections are required for the higher Mach numbers.

CONCLUSIONS

The following conclusions were drawn from the results of the investigation of a fighter model with closed and extended air brakes located close behind the wing on the fuselage:

1. The increment of drag coefficient of the model due to the extended brakes was about 0.03 up to a Mach number of about 0.94 and decreased to approximately 0.02 at a Mach number of 1.0 and above. The drag coefficient for an equivalent projected flat plate was estimated to be 0.045.

2. The effectiveness of the brakes was reduced due to their proximity to the wing.

3. The change of the static longitudinal stability resulting from the extended brakes required stabilizer changes of ±1° or less over the Mach number range investigated in order to maintain a trimmed lift coefficient of 0.2 or 0.3.

Langley Aeronautical Laboratory,
National Advisory Committee for Aeronautics,
Langley Field, Va., January 9, 1956.

REFERENCES

1. Stephenson, Jack D.: The Effects of Aerodynamic Brakes Upon the Speed Characteristics of Airplanes. NACA TN 1939, 1949.

2. Arabian, Donald D.: Effect of Large Negative Dihedral on the Horizontal Tail of the Longitudinal and Lateral Stability Characteristics of a Swept-Wing Configuration at Transonic Speeds. NACA RM L55I20, 1955.

3. Hallissy, Joseph M., Jr., and Kudlacik, Louis: A Transonic Wind-Tunnel Investigation of Store and Horizontal-Tail Loads and Some Effects of Fuselage-Afterbody Modifications on a Swept-Wing Fighter Airplane. NACA RM L56A26, 1956.

MODEL GEOMETRY

Wing
- Airfoil section normal to C/4 NACA 64A010
- Area excluding inlet extension.....6.63 sq ft
- Aspect ratio.....3.43
- Taper ratio.....0.578
- Sweep at C/4.....40°
- Incidence.....1.5°

Horizontal tail
- Area.....1.13 sq ft
- Aspect ratio.....3.59
- Taper ratio.....1.0
- Sweep.....40°

Vertical tail
- Area.....0.87 sq ft
- Aspect ratio.....1.68
- Taper ratio.....0.402
- Sweep C/4.....41.27°

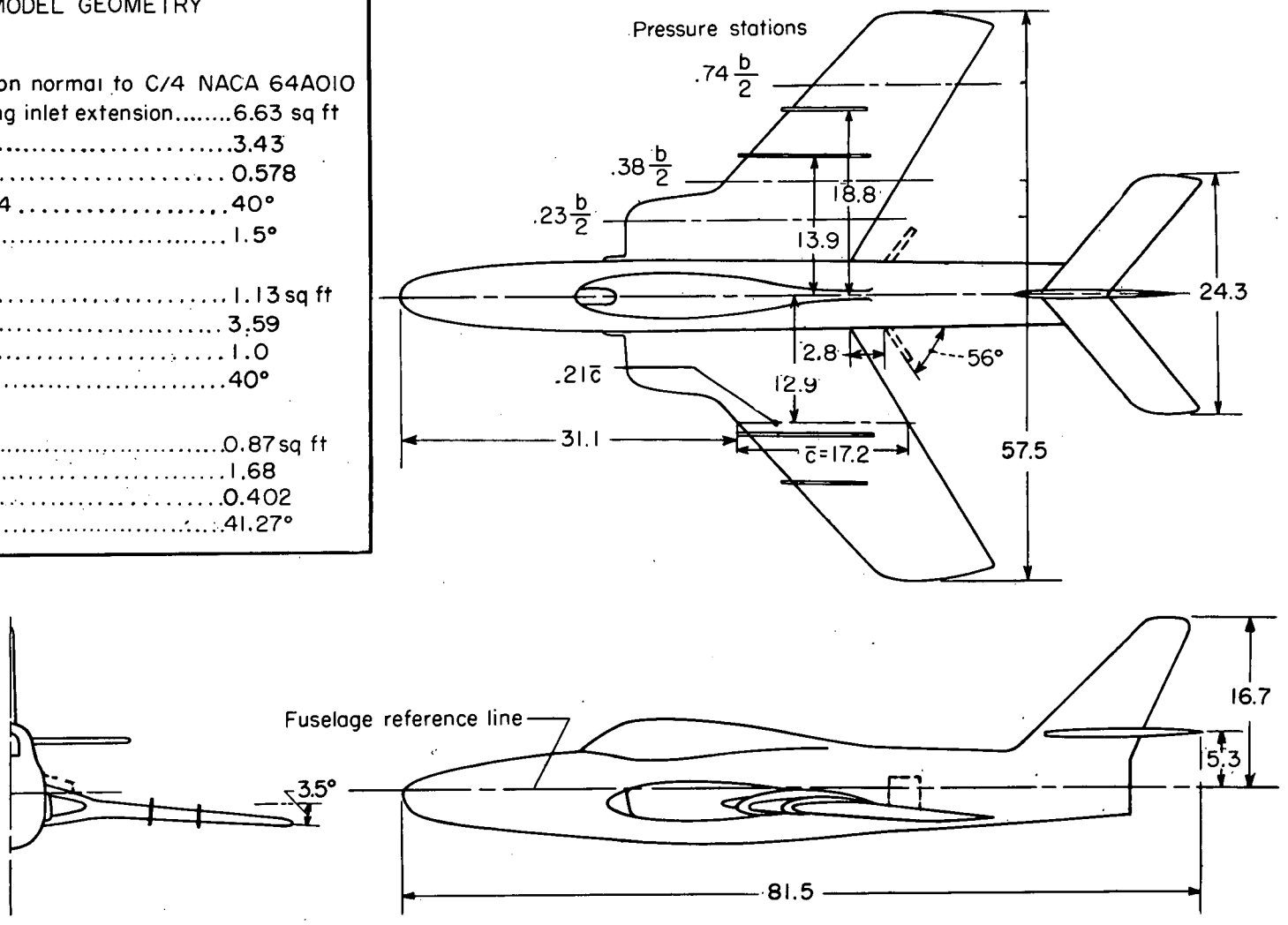

Figure 1.- General arrangement of model. All dimensions are in inches.

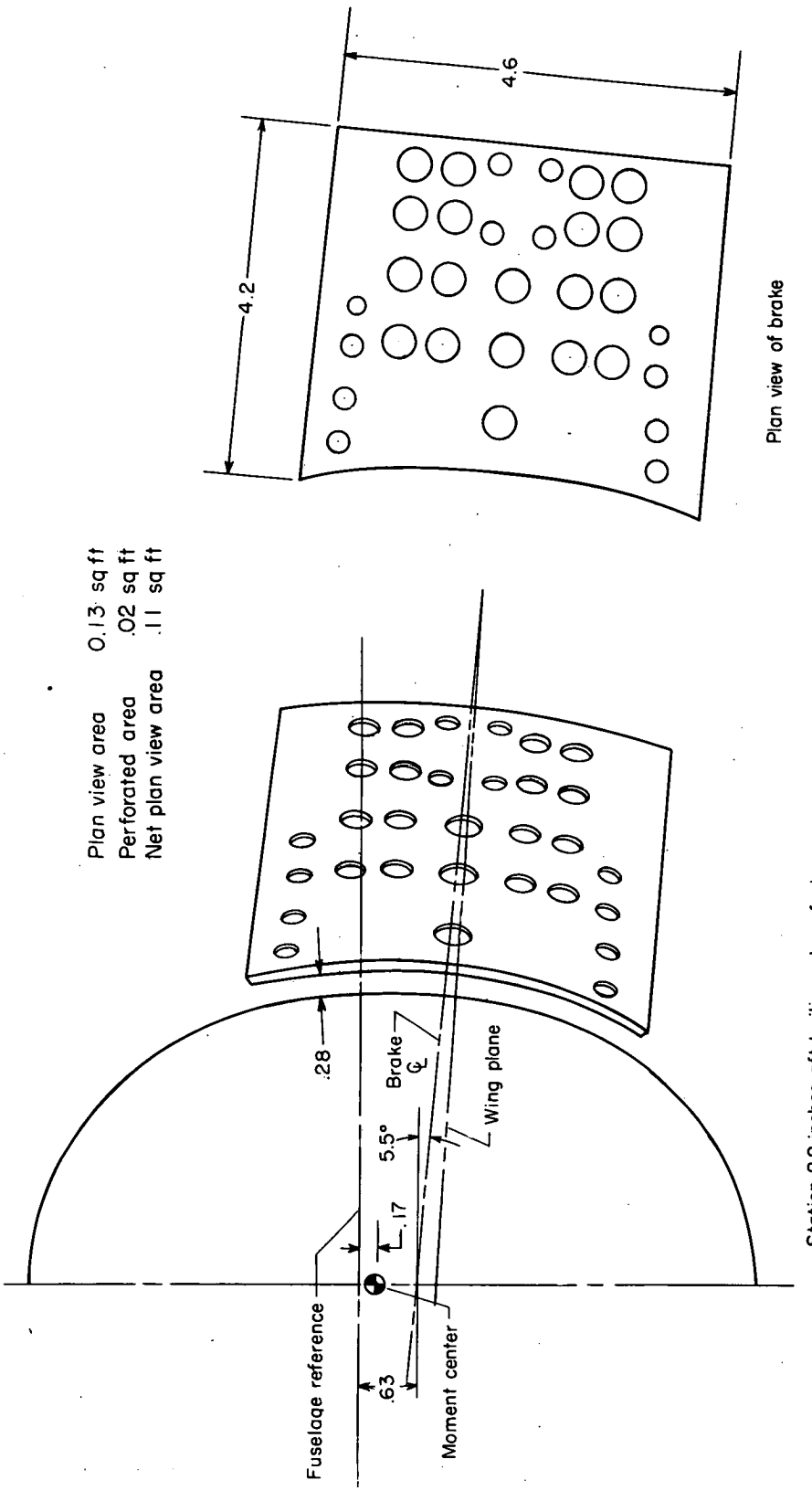

Figure 2.- Detail of air brake extended 56 degrees. All dimensions are in inches.

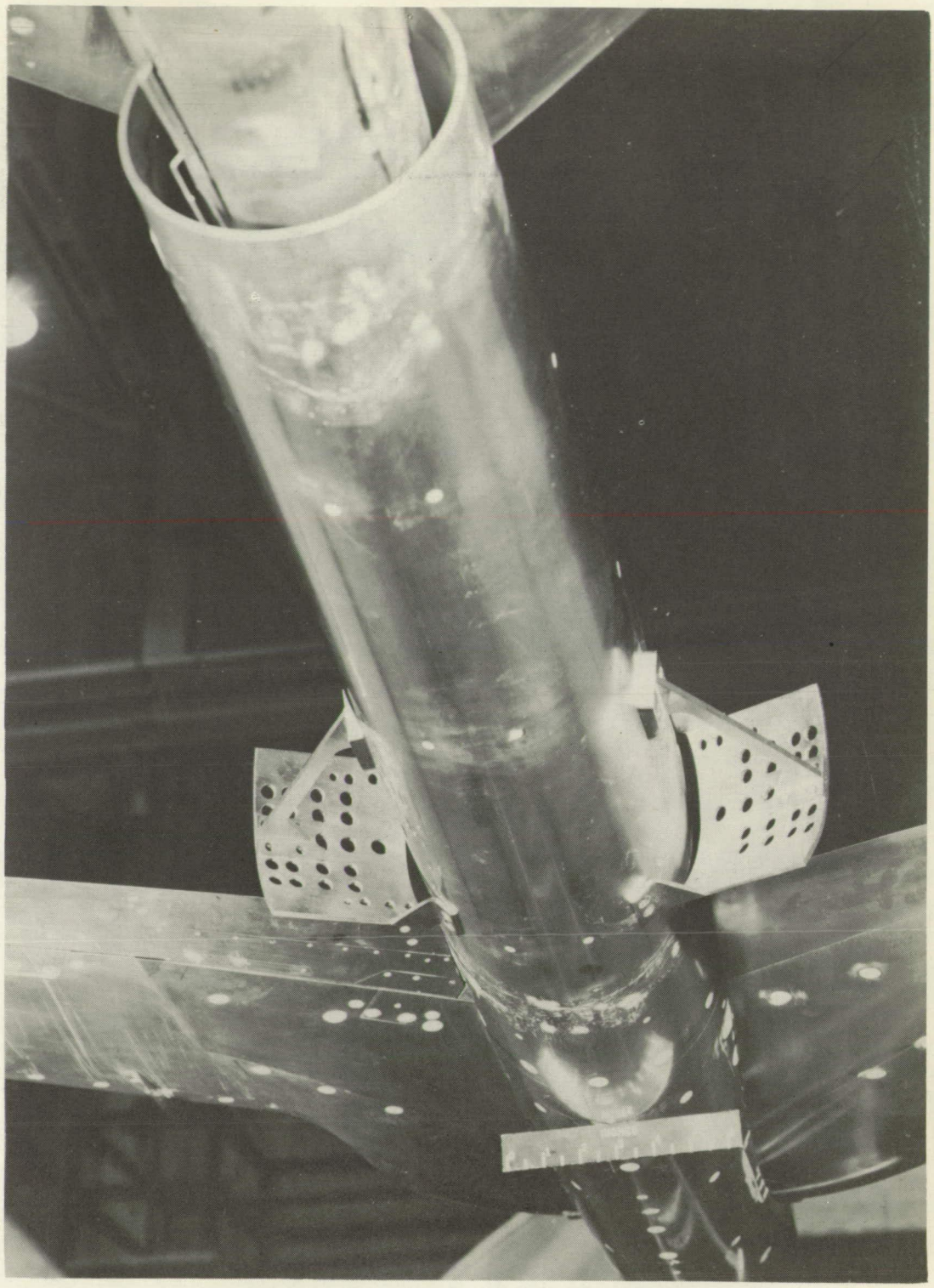

L-85431

Figure 3.- Rear view of the model with air brakes extended.

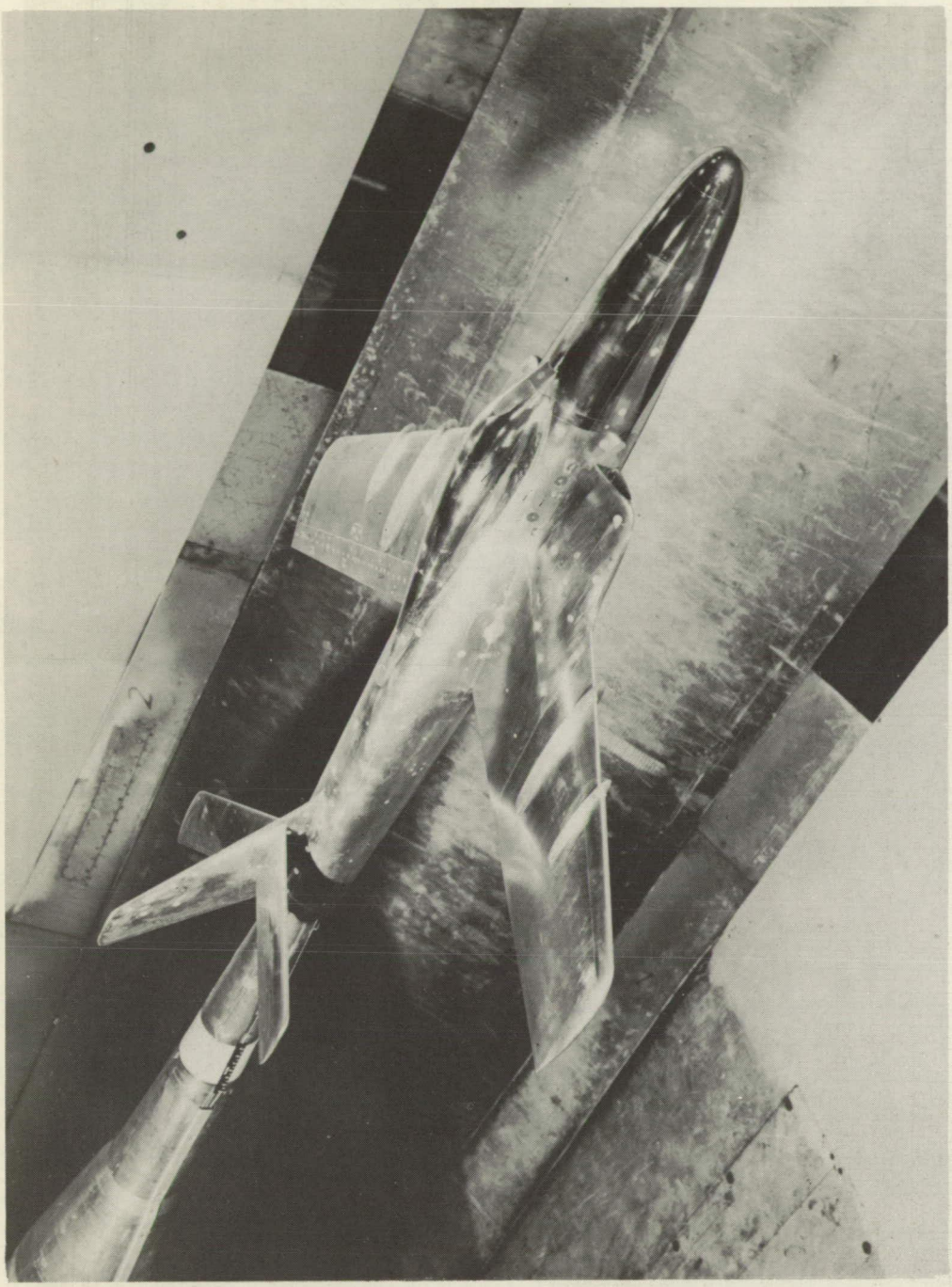

L-85379

Figure 4.- Model mounted in the Langley 16-foot transonic tunnel with closed air brakes.

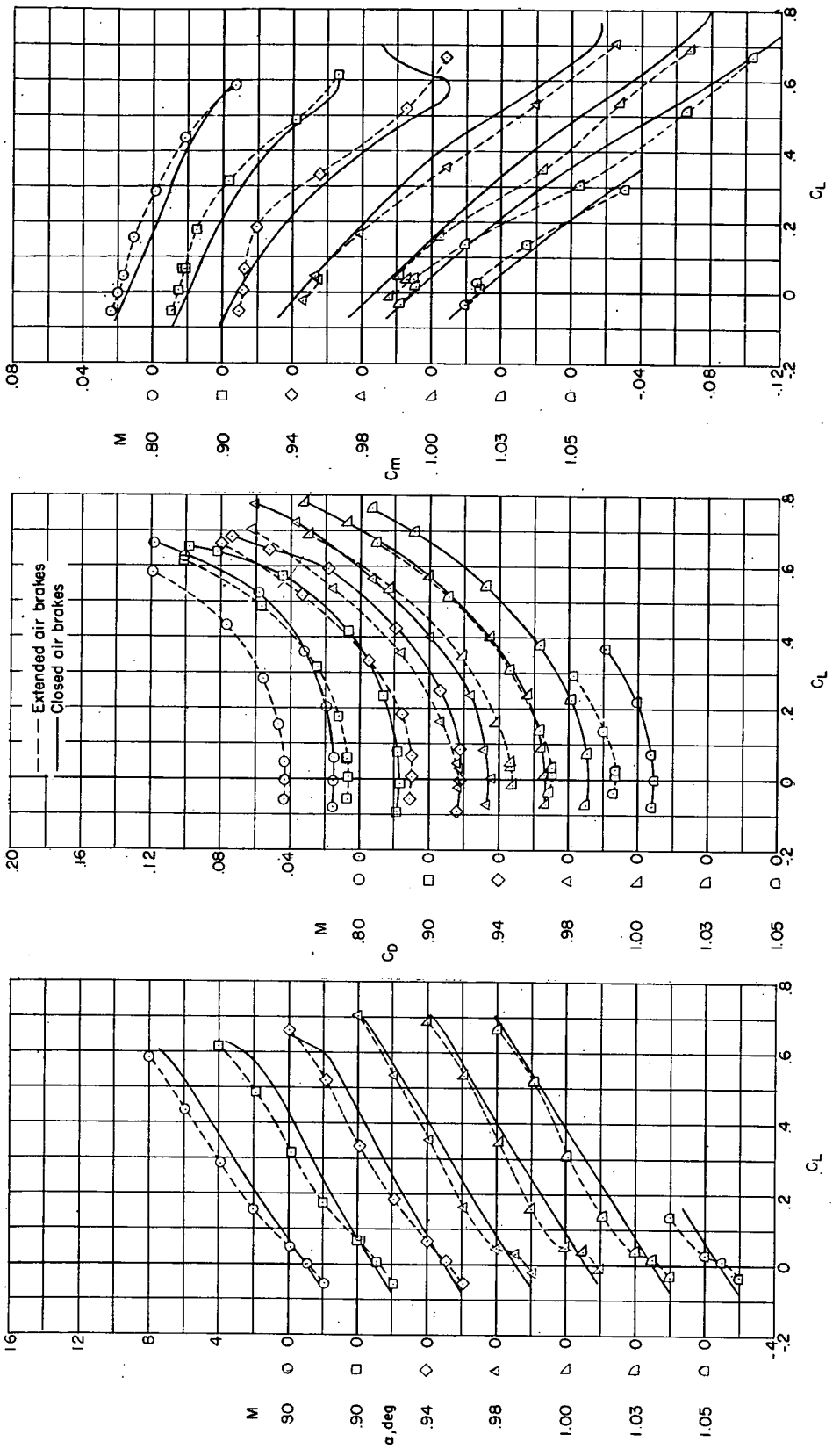

(a) Lift coefficient. (b) Drag coefficient. (c) Pitching-moment coefficient.

Figure 5.- Lift, drag and pitching-moment characteristics of the model with extended and closed air brakes.

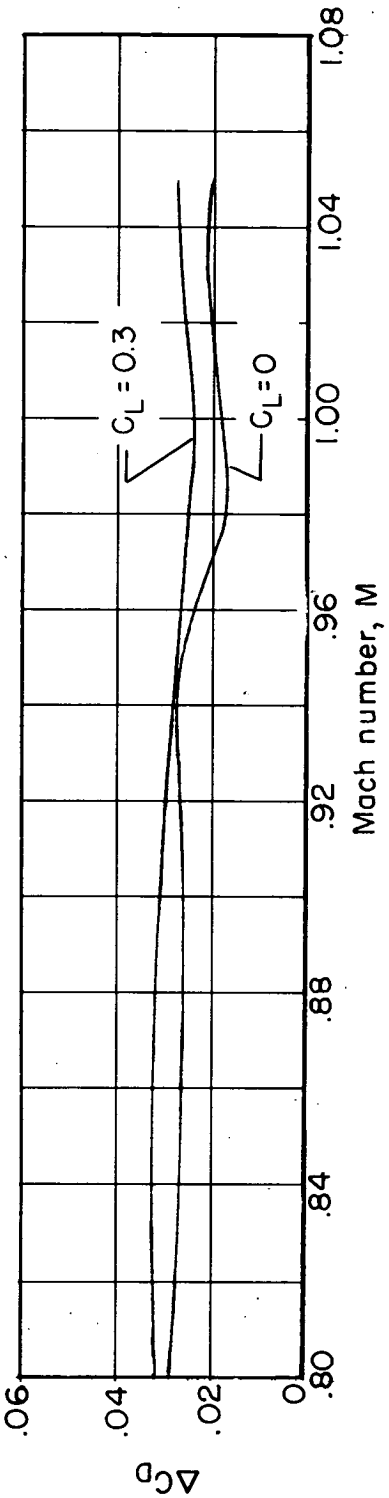

(a) Increment of drag coefficient.

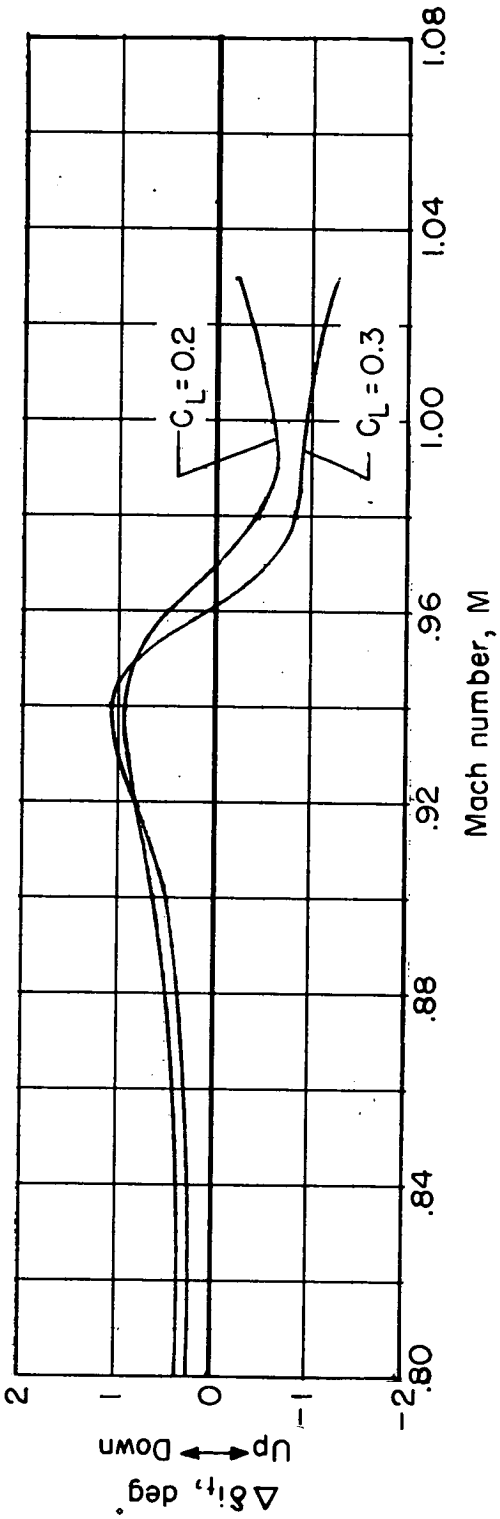

(b) Change of elevator setting.

Figure 6.- Effect of extended air brakes on C_D and elevator setting for constant C_L values.

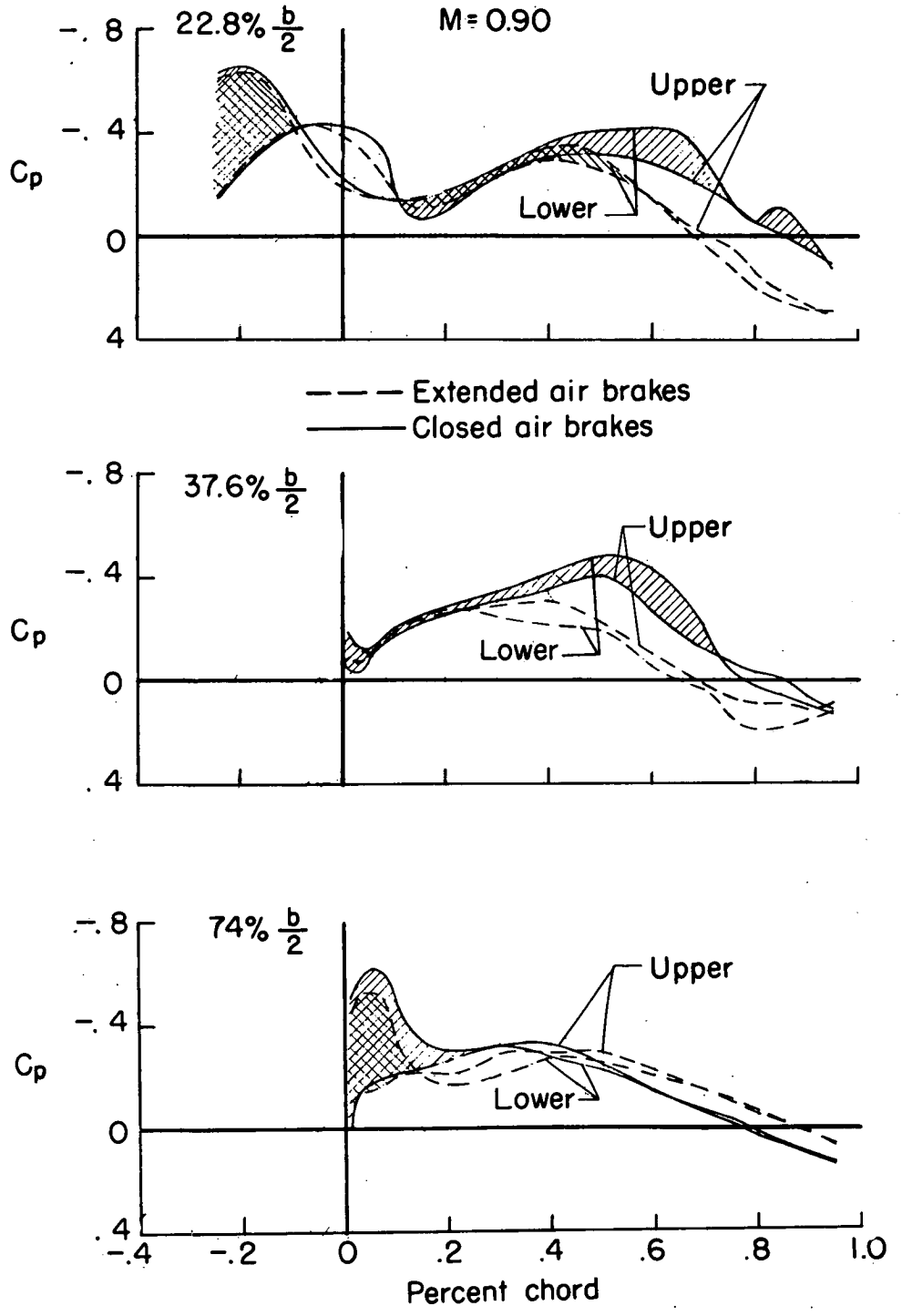

(a) $\alpha = -2^{\circ}$; M = 0.90.

Figure 7.- Chordwise pressure distributions for three spanwise stations for the model with extended and closed air brakes. Shaded areas indicate negative lift.

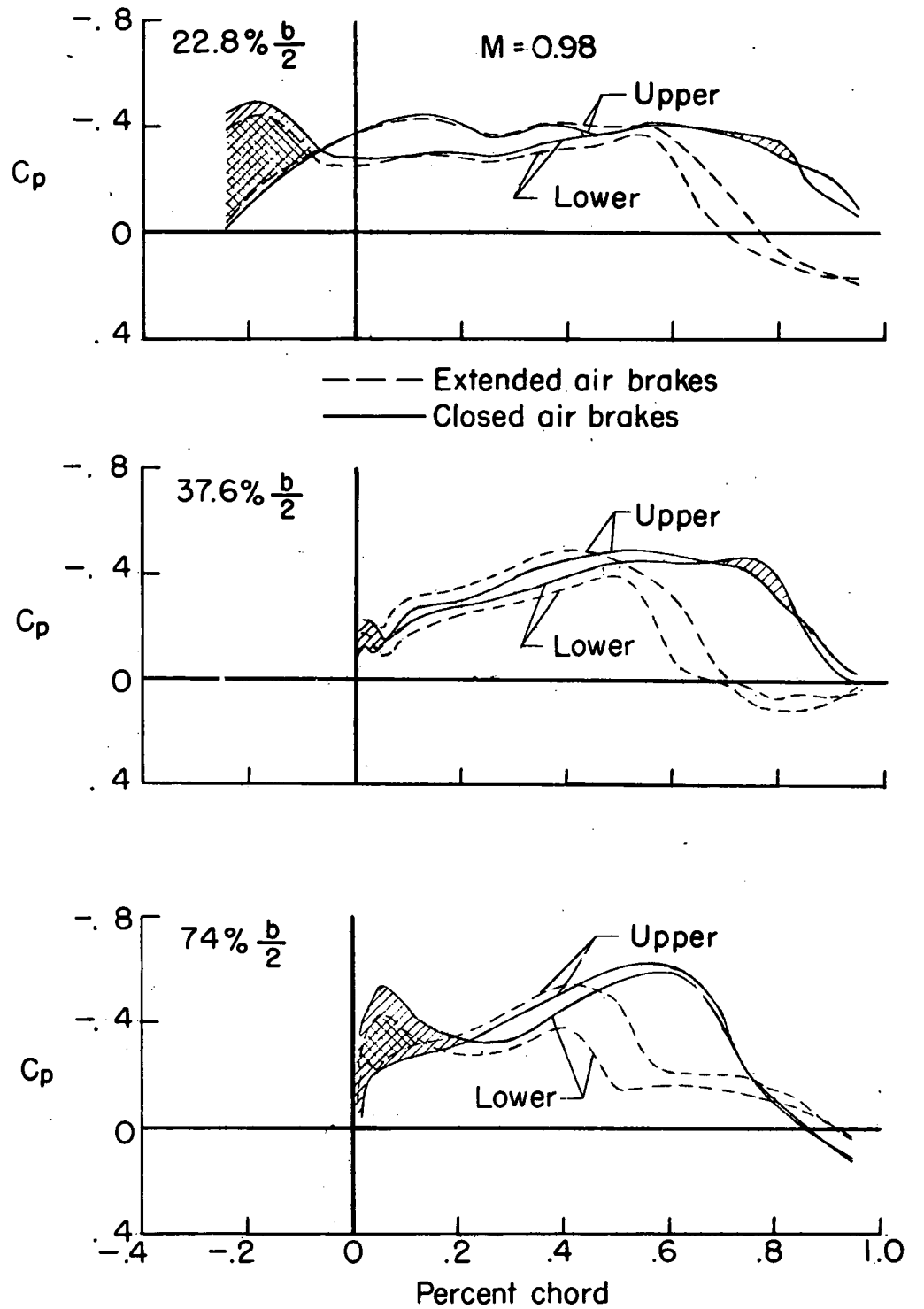

(a) $\alpha = -2^{\circ}$; M = 0.98. Continued.

Figure 7.- Continued.

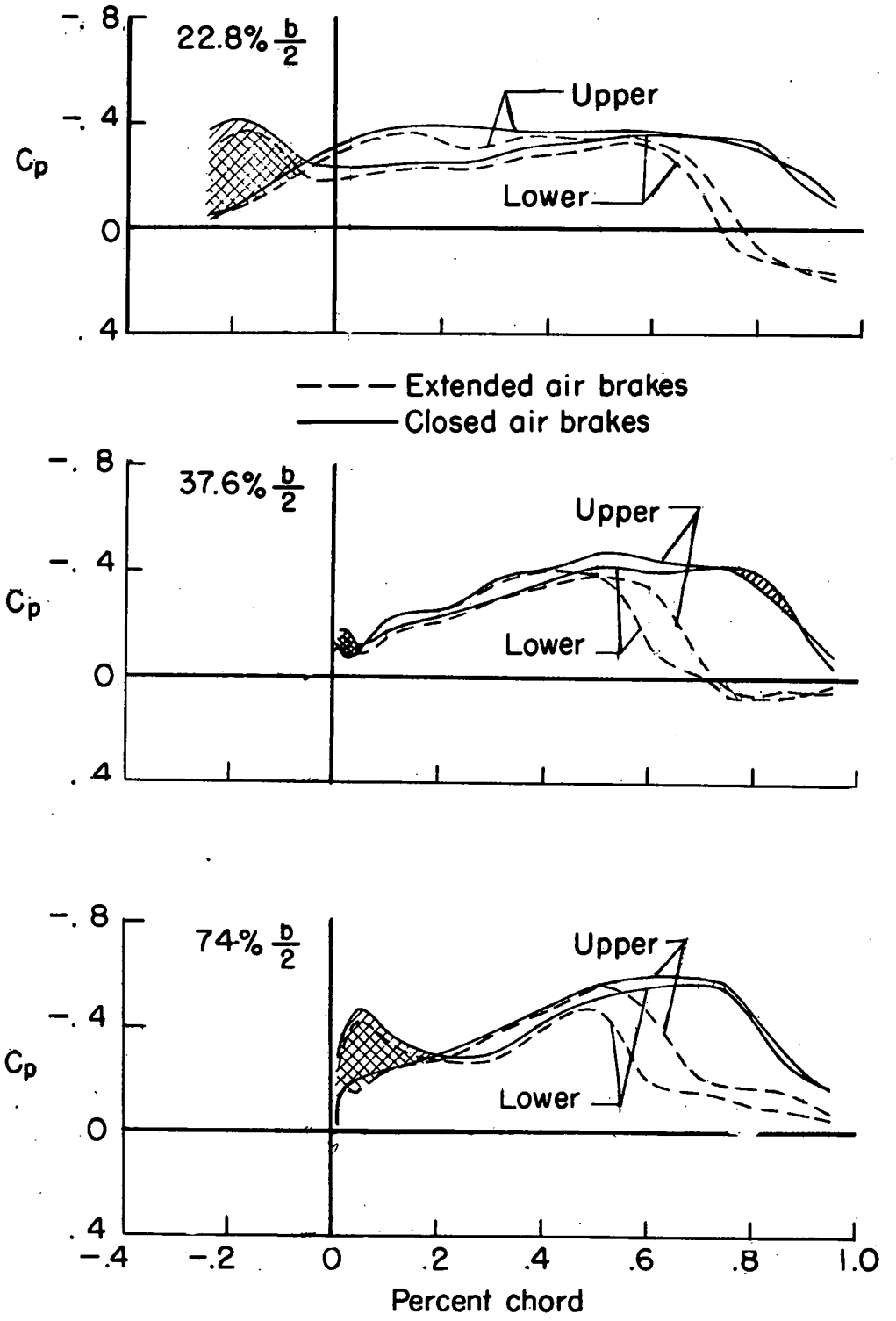

(a) $\alpha = -2^{\circ}$; M = 1.03. Concluded.

Figure 7.- Continued.

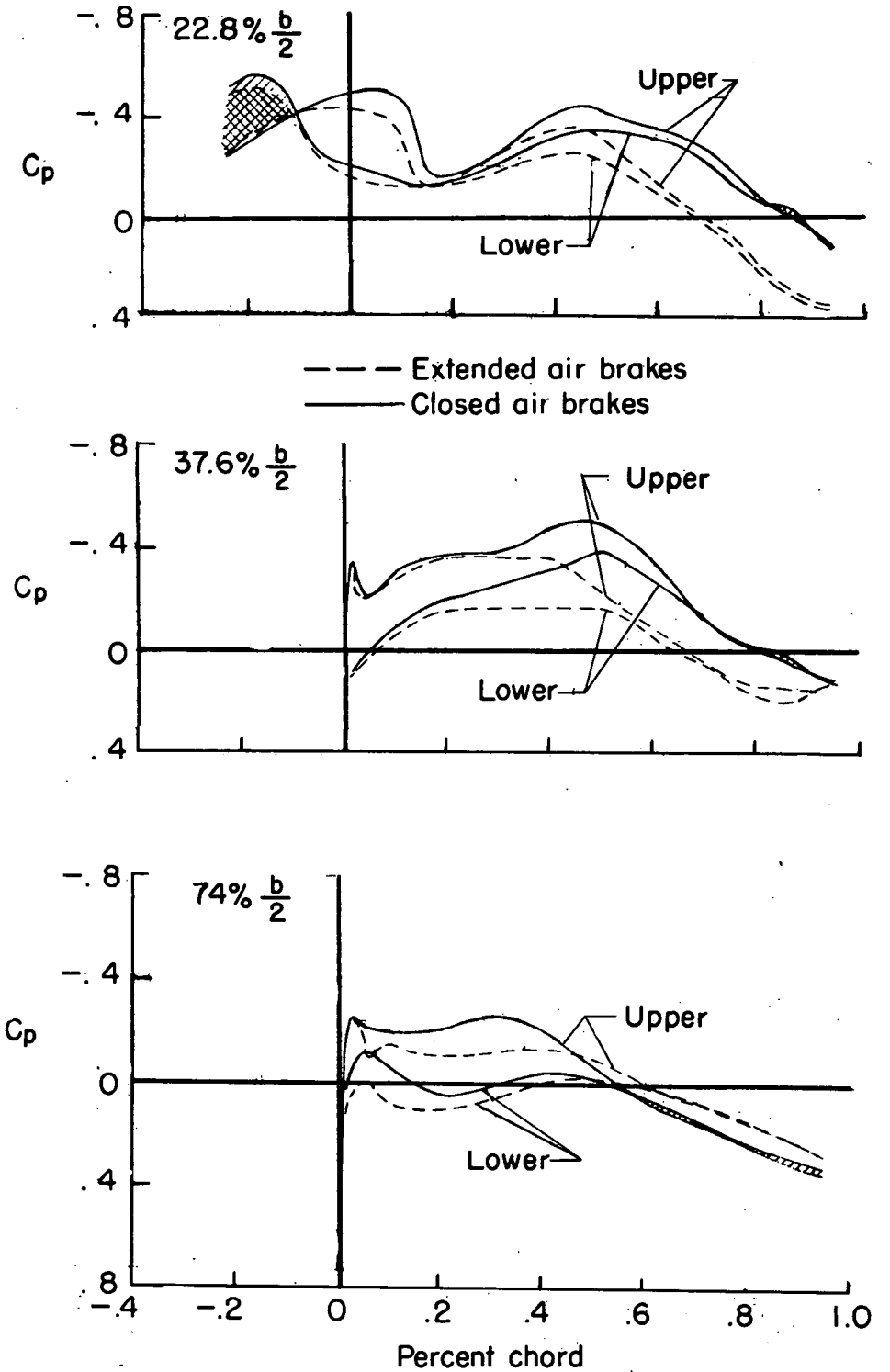

(b) $\alpha = 0^{\circ}$; M = 0.90.

Figure 7.- Continued.

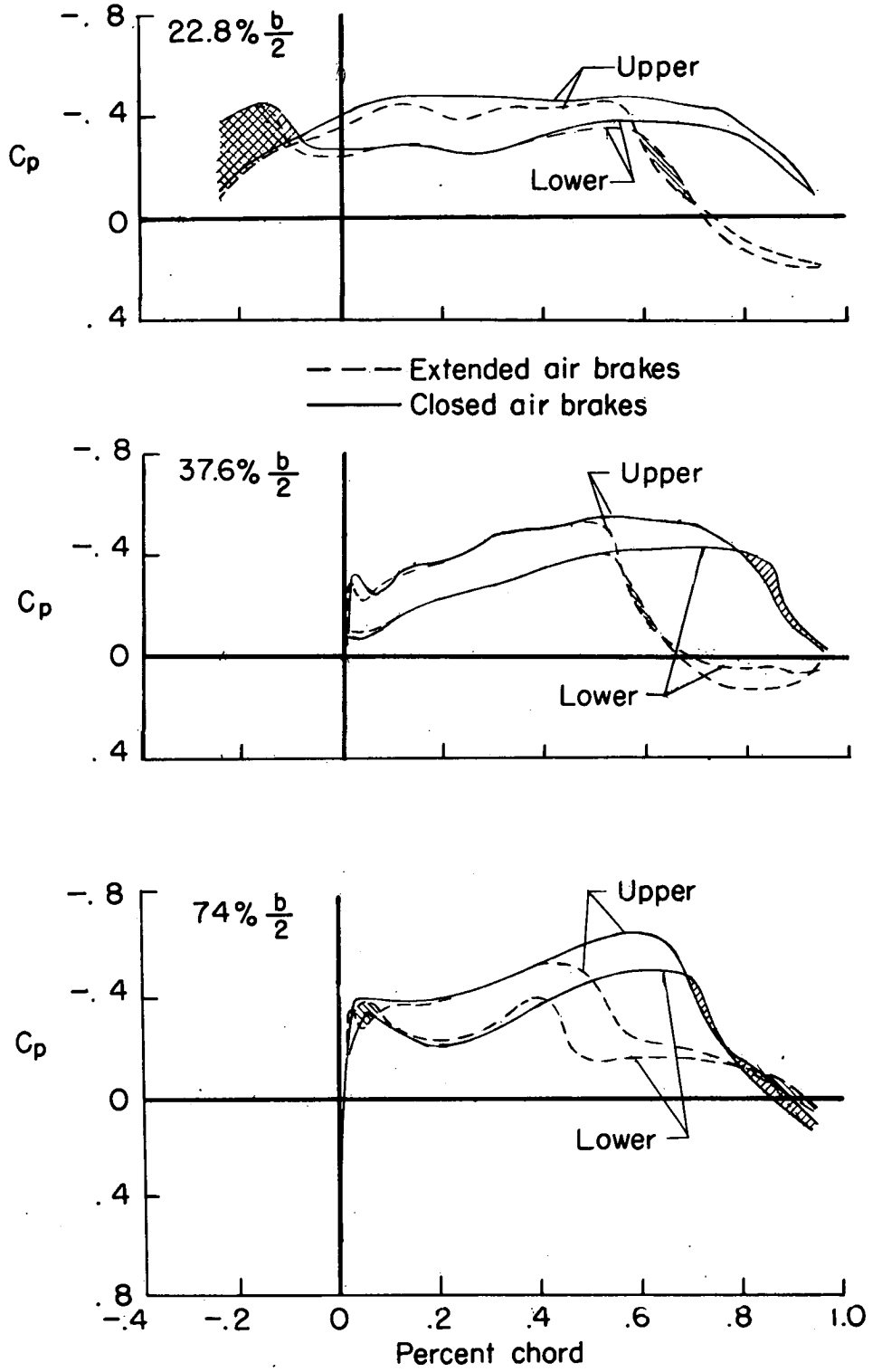

(b) $\alpha = 0^{\circ}$; M = 0.98. Continued.

Figure 7.- Continued.

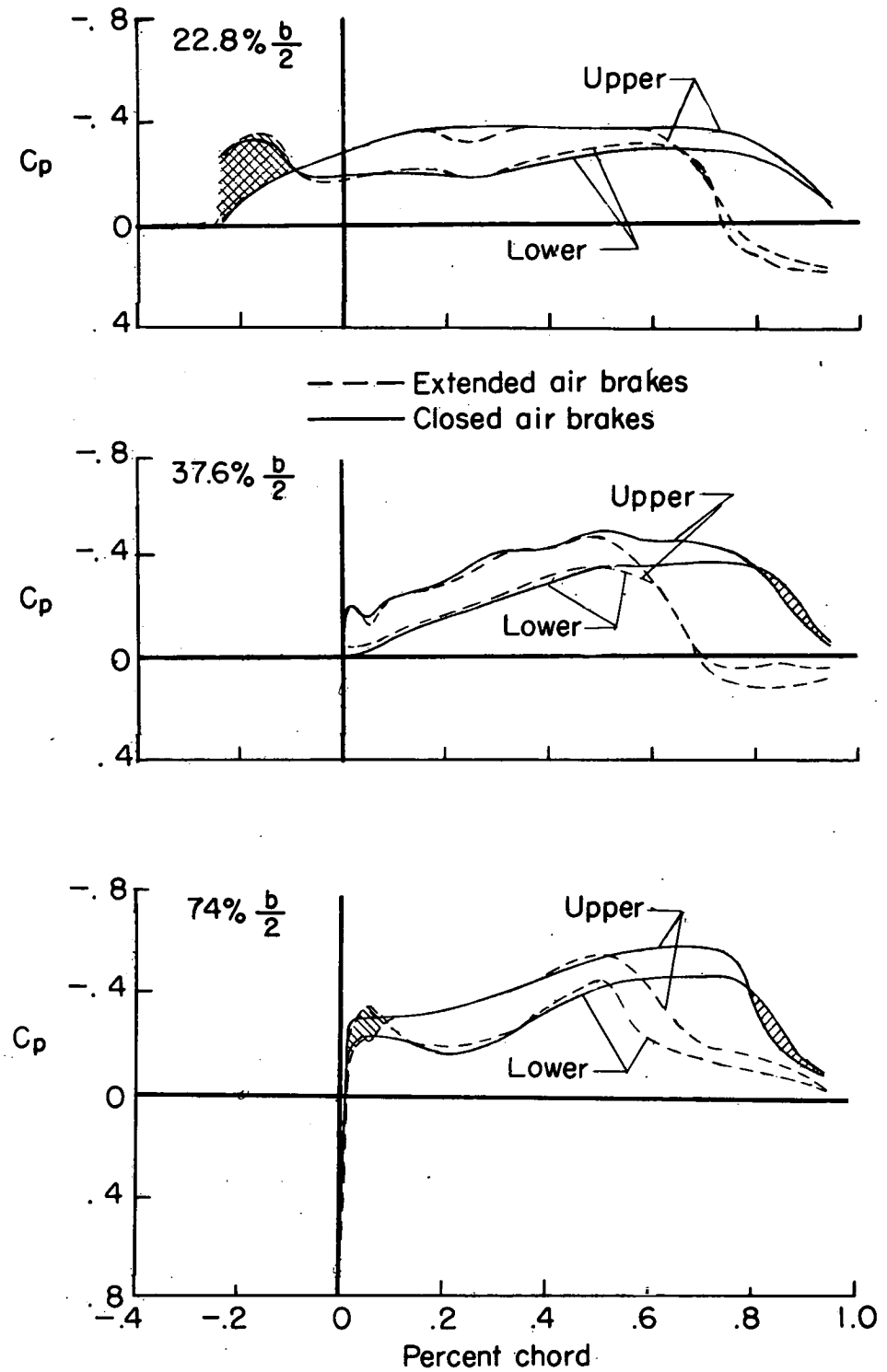

(b) $\alpha = 0^{\circ}$; M = 1.03. Concluded.

Figure 7.- Continued.

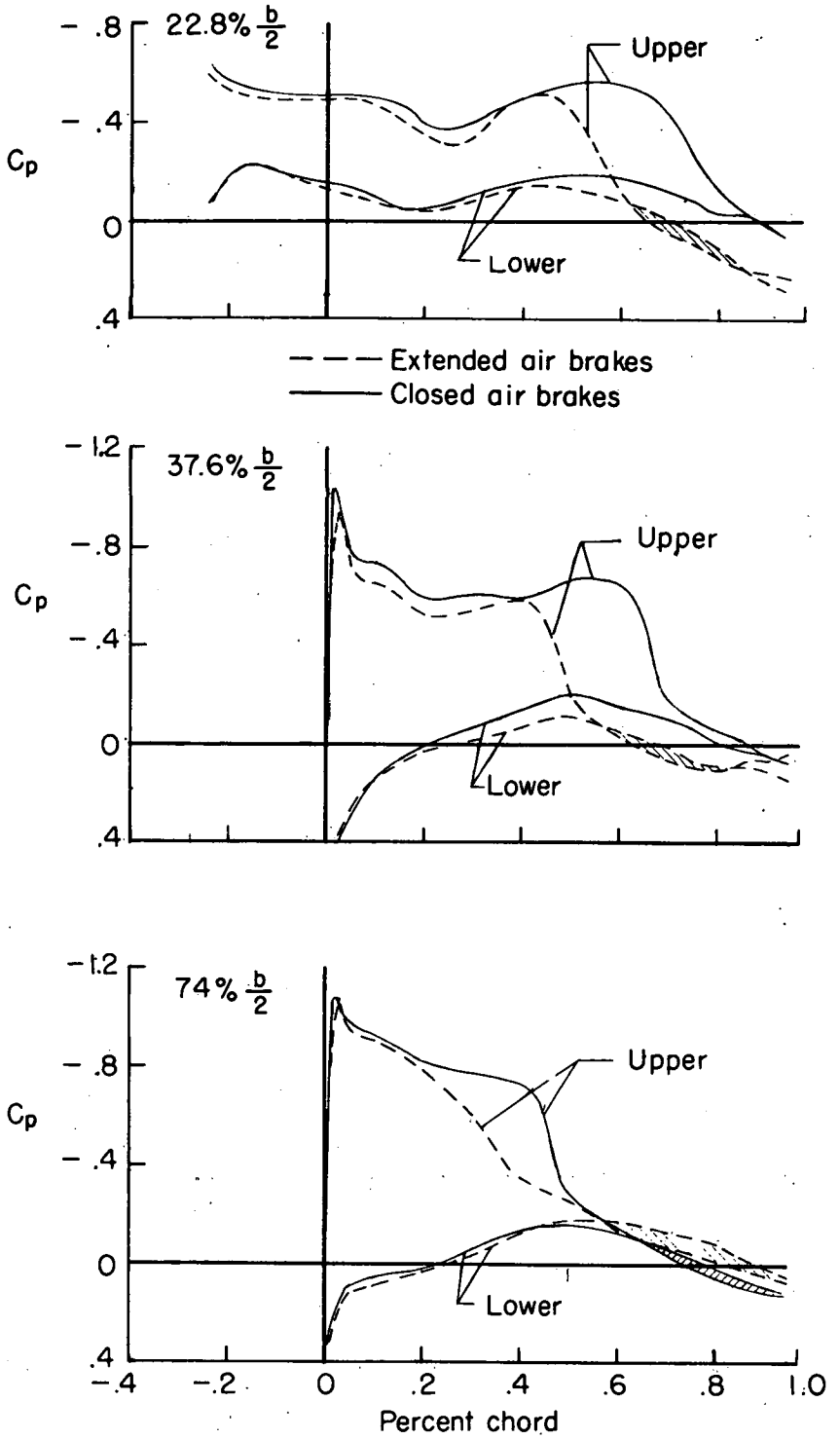

(c) $\alpha = 4^{\circ}$; $M = 0.90$.

Figure 7.- Continued.

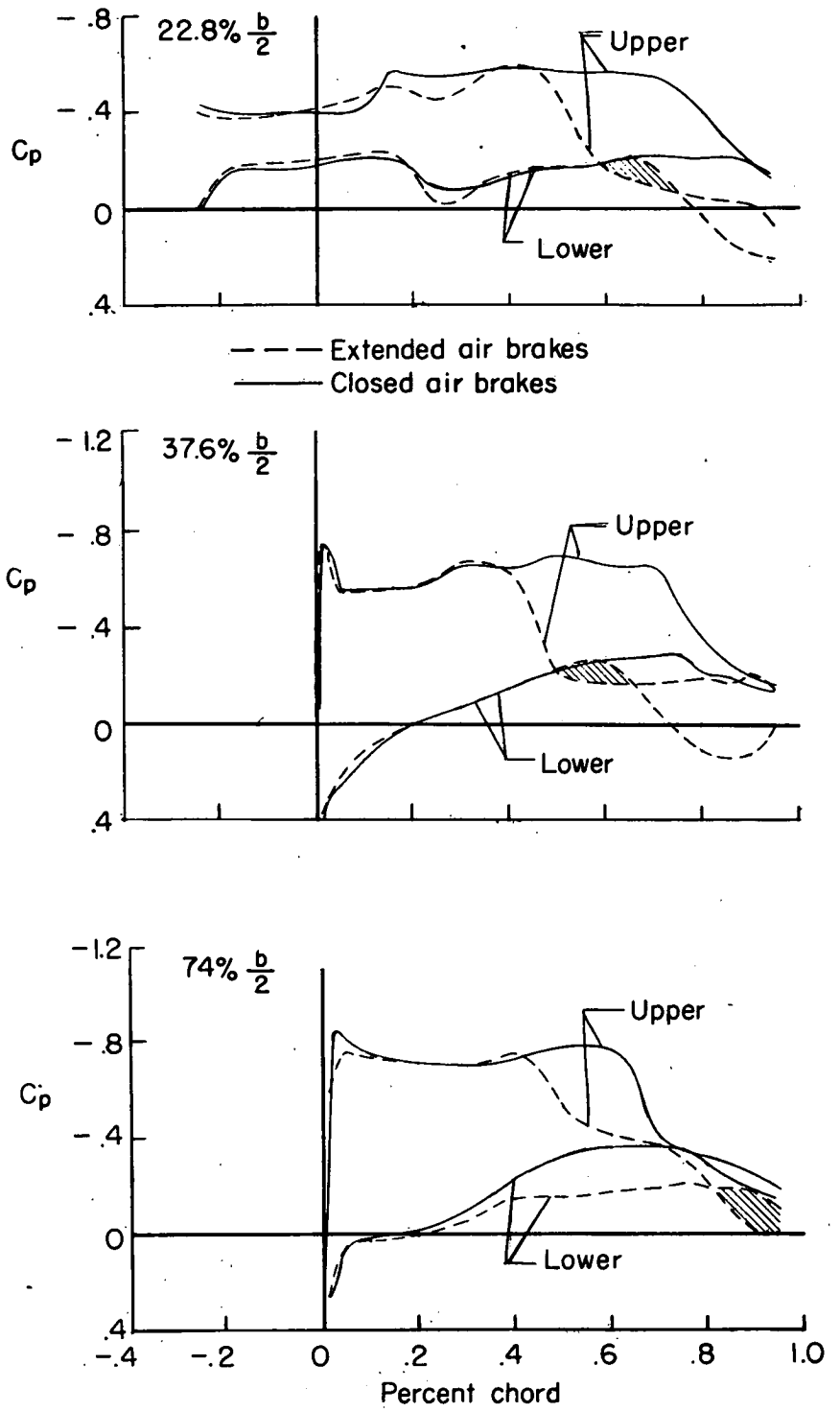

(c) $\alpha = 4^{\circ}$; M = 0.98. Continued.

Figure 7.- Continued.

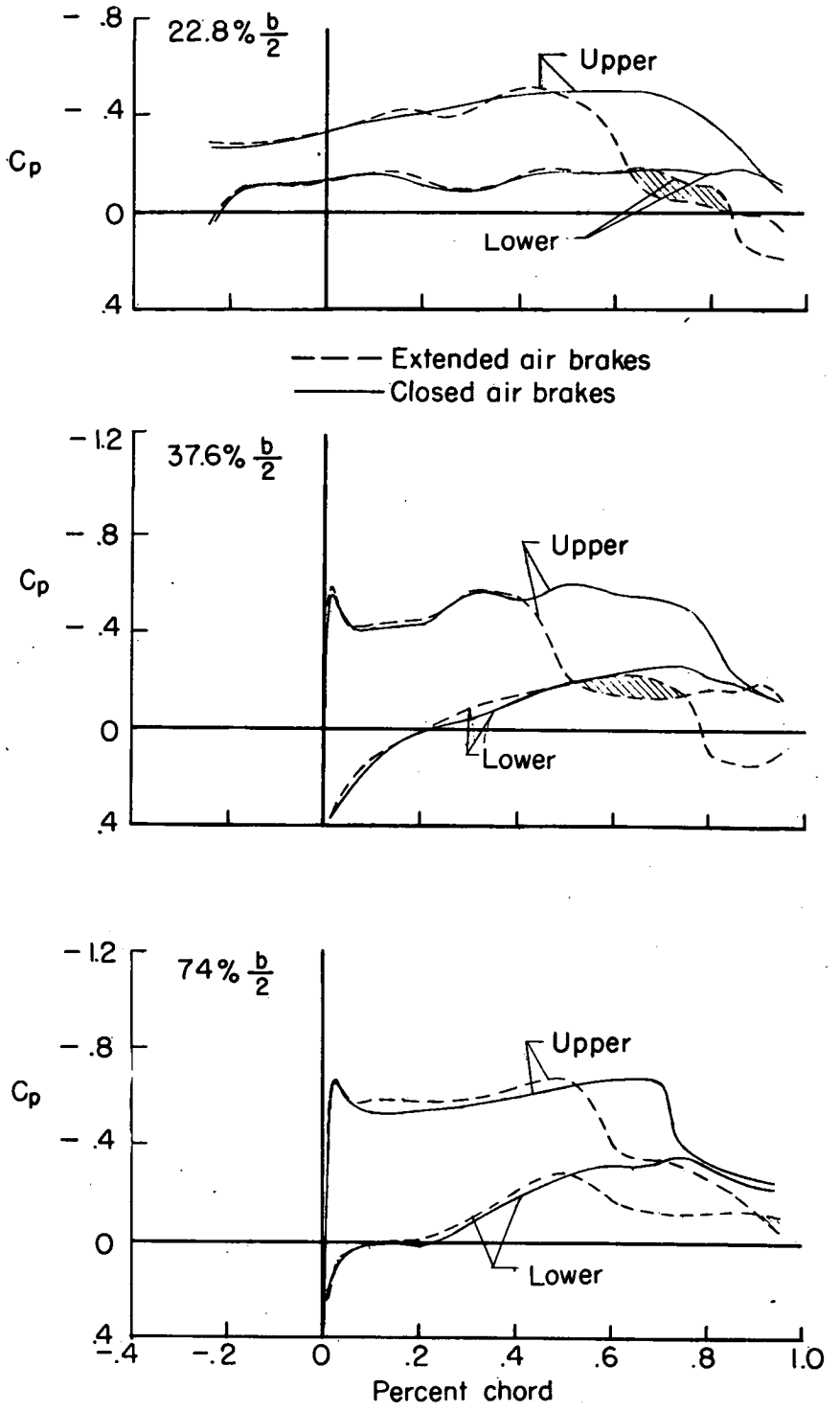

(c) $\alpha = 4^{\circ}$; M = 1.03. Concluded.

Figure 7.- Concluded.

NACA - Langley Field, Va.